Hadronic Vacuum Polarization and Two-Photon Excitations in Highly Charged Ions

Eugen Dizer

Heidelberg University

December 6, 2022

Outline

1. One-Loop QED Corrections

Outline

1. One-Loop QED Corrections
2. Hadronic Vacuum Polarization
   - Hadronic Uehling Potential
   - Energy Level Correction
   - g Factor Correction

Outline

1. One-Loop QED Corrections
2. Hadronic Vacuum Polarization
   - Hadronic Uehling Potential
   - Energy Level Correction
   - g Factor Correction
3. Two-Photon Excitations
   - Rabi Frequency
   - Cross Section

Outline

1. One-Loop QED Corrections
2. Hadronic Vacuum Polarization
   - Hadronic Uehling Potential
   - Energy Level Correction
   - g Factor Correction
3. Two-Photon Excitations
   - Rabi Frequency
   - Cross Section
4. Outlook

Outline

1. One-Loop QED Corrections
2. Hadronic Vacuum Polarization
   - Hadronic Uehling Potential
   - Energy Level Correction
   - g Factor Correction
3. Two-Photon Excitations
   - Rabi Frequency
   - Cross Section
4. Outlook

Quantum Electrodynamics (QED)

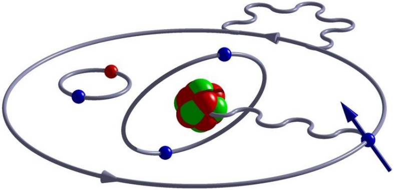

Figure: Scheme of the QED contributions to the electronic structure of highly charged ions.[1]

$$\mathcal{L}_{\mathrm{QED}} = \bar{\psi}\left[\gamma^{\mu}\left(i\hbar c\partial_{\mu} - eA_{\mu}\right) - m_e c^2\right]\psi - \frac{1}{16\pi}F_{\mu\nu}F^{\mu\nu}\,. \tag{1}$$

[1] https://www.mpi-hd.mpg.de/mpi/fileadmin/bilder/Progress_Reports/2017-19/2QuantumDynamics.pdf

Energy Level Corrections

Vacuum Polarization:

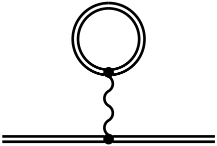

Self-Energy Correction:

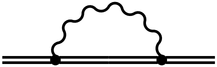

Energy Level Corrections

Vacuum Polarization:

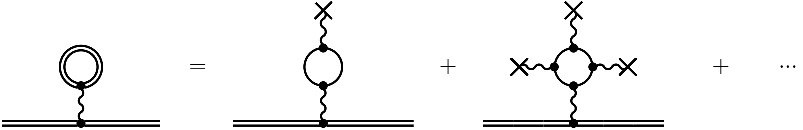

Modification of the Photon Propagator[1]:

$$= \quad iD_{\mu\nu}(k) \quad + \quad iD_{\mu\lambda}(k)\frac{i\Pi^{\lambda\sigma}(k)}{4\pi}iD_{\sigma\nu}(k)$$

[1] Inspired by W. Greiner and J. Reinhardt, Quantum Electrodynamics (2009).

g Factor Corrections

Describes the coupling of the electron's magnetic moment $\boldsymbol{\mu}$ to its total angular momentum $\boldsymbol{J}$.
Interaction with an external homogeneous magnetic field $\boldsymbol{B}$:

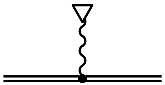

First-order Zeeman splitting:

$$\Delta E = - \langle \boldsymbol{\mu} \cdot \boldsymbol{B} \rangle = g \mu_{\mathrm{B}} \langle \boldsymbol{J} \cdot \boldsymbol{B} \rangle \,, \tag{2}$$

where $\mu_{\mathrm{B}} = \sqrt{\pi\alpha}/m_e$ is the Bohr magneton of the electron.

g Factor Corrections

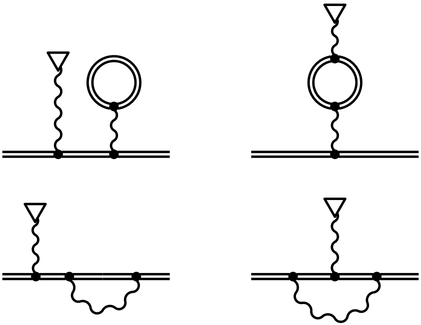

Figure: Feynman diagrams representing the first-order radiative corrections to the g factor of the bound electron.

Outline

1 One-Loop QED Corrections

2 Hadronic Vacuum Polarization
- Hadronic Uehling Potential
- Energy Level Correction
- g Factor Correction

3 Two-Photon Excitations
- Rabi Frequency
- Cross Section

4 Outlook

Hadronic Vacuum Polarization

Hadronic Polarization Function through measured cross section

$\sigma_{e^+e^- \to \text{ hadrons}}$

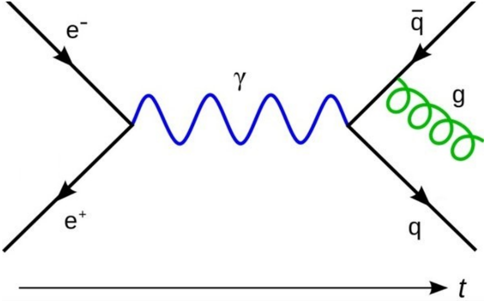

Figure: Feynman diagram representing the annihilation of e^+e^- into hadrons[1].

[1] https://www.pngitem.com/middle/ihmixmR_electron-positron-to-quark-antiquark-hd-png-download/

Hadronic Vacuum Polarization

Real Part of the Hadronic Polarization Function[1]:

$$\mathrm{Re}\left[\Pi_{\mathrm{had}}(q^2)\right] = A_i + B_i \ln(1 + C_i q^2), \tag{3}$$

The parameters are given by

i	Region	Range [GeV]	A_i	B_i	C_i [GeV^{-2}]
1	0 - k_1	0.0 - 0.7	0.0	0.0023092	3.9925370
2	k_1 - k_2	0.7 - 2.0	0.0	0.0022333	4.2191779
3	k_2 - k_3	2.0 - 4.0	0.0	0.0024402	3.2496684
4	k_3 - k_4	4.0 - 10.0	0.0	0.0027340	2.0995092
5	k_4 - k_5	10.0 - m_Z	0.0010485	0.0029431	1.0
6	k_5 - k_6	m_Z - 10^4	0.0012234	0.0029237	1.0
7	k_5 - k_6	10^4 - 10^5	0.0016894	0.0028984	1.0

[1] H. Burkhardt and B. Pietrzyk, Physics Letters B 513, 46–52 (2001).

Hadronic Uehling Potential

Numerical Hadronic Uehling Potential for a point-like Nucleus:

$$\delta V^{\text{had. VP}}_{\text{numerical}}(r) = -\frac{2Z\alpha}{\pi} \sum_{k=1}^{7} \int_{k_{i-1}}^{k_i} dq \, \frac{\sin(qr)}{qr} \left[A_i + B_i \ln(1 + C_i q^2)\right] . \quad (4)$$

Analytical Hadronic Uehling Potential for a point-like Nucleus[1]:

$$\begin{aligned} \delta V^{\text{had. VP}}_{\text{analytical}}(r) &= -\frac{2Z\alpha}{\pi} \int_0^{\infty} dq \, \frac{\sin(qr)}{qr} \left[A_1 + B_1 \ln(1 + C_1 q^2)\right] \\ &= -\frac{2Z\alpha}{r} B_1 \, \mathrm{E}_1\left(\frac{r}{\sqrt{C_1}}\right) . \end{aligned} \quad (5)$$

[1] S. Breidenbach et al., Physical Review A 106, 042805 (2022).

Hadronic Uehling Potential

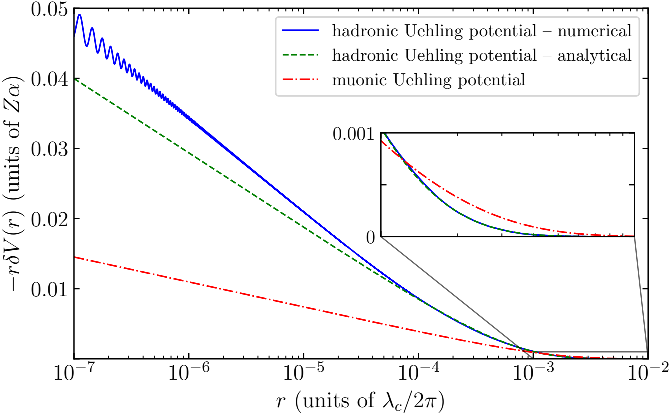

Figure: Comparison of muonic and hadronic Uehling potential[1].

[1] S. Breidenbach et al., Physical Review A 106, 042805 (2022).

Hadronic Energy Shift

Relativistic Energy Shift of the $1s$ State for a point-like Nucleus:

$$\Delta E_{1s}^{\text{had. VP}} = \left\langle \delta V^{\text{had. VP}} \right\rangle_{1s}$$
$$= -\frac{Z\alpha\lambda(2\lambda\sqrt{C_1})^{2\gamma} B_1}{\gamma^2} \; {}_2F_1\left(2\gamma, 2\gamma; 1+2\gamma; -2\lambda\sqrt{C_1}\right), \quad (6)$$

with $\lambda = Z\alpha m_e$ and $\gamma = \sqrt{1-(Z\alpha)^2}$.

$Z\alpha$ Expansion:

$$\Delta E_{1s}^{\text{had. VP}} \approx -4B_1 C_1 m_e^3 (Z\alpha)^4 + \frac{32 B_1 C_1^{3/2} m_e^4 (Z\alpha)^5}{3}$$
$$-4B_1 C_1 m_e^3 (Z\alpha)^6 \left[1 + 6C_1 m_e^2 - \ln(2Z\alpha\sqrt{C_1} m_e)\right]. \quad (7)$$

Hadronic Energy Shift

For comparison: Leptonic VP $\Delta E^{\text{point}}_{e^+e^-}(Z=1) = -8.975 \cdot 10^{-7}$ eV.

Z	$\Delta E^{\text{point}}_{\text{analytical}}$ [eV]	$\Delta E^{\text{point}}_{\text{numerical}}$ [eV]	$\Delta E^{\text{finite size}}_{\text{exact}}$ [eV]
1	$-1.3963 \cdot 10^{-11}$	$-1.39(33) \cdot 10^{-11}$	$-1.391(4) \cdot 10^{-11}$
14	$-5.9178 \cdot 10^{-7}$	$-5.90(18) \cdot 10^{-7}$	$-5.756(1) \cdot 10^{-7}$
20	$-2.7133 \cdot 10^{-6}$	$-2.71(5) \cdot 10^{-6}$	$-2.5596(3) \cdot 10^{-6}$
70	$-3.1090 \cdot 10^{-3}$	$-3.109(4) \cdot 10^{-3}$	$-1.248(1) \cdot 10^{-3}$
82	$-1.4128 \cdot 10^{-2}$	$-1.413(1) \cdot 10^{-2}$	$-3.693(4) \cdot 10^{-3}$

Table: Energy shifts due to hadronic VP[1].

[1] E. Dizer, Bachelor Thesis, Heidelberg University (2020).

Hadronic g Factor Shift

Relativistic g Factor Shift of the $1s$ State for a point-like Nucleus[1]:

$$\Delta g_{1s}^{\text{had. VP}} = -\frac{4}{3m_e}\left\langle r\frac{\partial \delta V^{\text{had. VP}}}{\partial r}\right\rangle_{1s}$$
$$= -\frac{8B_1(Z\alpha)^2(2\lambda\sqrt{C_1})^{2\gamma}}{3\gamma(1+2\lambda\sqrt{C_1})^{2\gamma}} + \frac{4}{3m_e}\Delta E_{1s}^{\text{had. VP}}. \qquad (8)$$

$Z\alpha$ Expansion:

$$\Delta g_{1s}^{\text{had. VP}} \approx -16B_1C_1m_e^2(Z\alpha)^4 + \frac{512B_1C_1^{3/2}m_e^3(Z\alpha)^5}{9}$$
$$-\frac{16B_1C_1m_e^2(Z\alpha)^6}{3}\left[2+30C_1m_e^2-3\ln(2m_eZ\alpha\sqrt{C_1})\right]. \qquad (9)$$

[1] S. G. Karshenboim et al., Physical Review A 72, 042101 (2005).

Hadronic g Factor Shift

Approximate formula in terms of Energy Shift:

$$\Delta g^{\text{had. VP}}_{\text{1s, approx}} \approx \frac{4(1+2\gamma)}{3m_e} \Delta E^{\text{had. VP}}_{\text{1s}} . \tag{10}$$

Isotopic shift[1]:

$^{20}\mathrm{Ne}^{9+}$: $R_{\text{rms}} = 3.0055(21)$ fm
$^{22}\mathrm{Ne}^{9+}$: $R_{\text{rms}} = 2.9525(40)$ fm

$$\Delta g^{\text{had. VP}}_{\text{rel., fns}} \left(1s, {}^{20}\mathrm{Ne}^{9+}\right) = -1.133(14) \times 10^{-12} \, , \tag{11}$$

$$\Delta g^{\text{had. VP}}_{\text{rel., fns}} \left(1s, {}^{22}\mathrm{Ne}^{9+}\right) = -1.133(15) \times 10^{-12} \, . \tag{12}$$

[1] T. Sailer et al., Nature 606, 479–483 (2022).

Hadronic g Factor Shift

For comparison: Leptonic VP $\Delta g^{\text{point}}_{e^+e^-}(Z=1) = -7.035 \cdot 10^{-12}$.

Z	$\Delta g^{\text{point}}_{\text{analytical}}$	$\Delta g^{\text{point}}_{\text{numerical}}$	$\Delta g^{\text{finite size}}_{\text{approx}}$
1	$-1.0929 \cdot 10^{-16}$	$-1.09(9) \cdot 10^{-16}$	$-1.09(2) \cdot 10^{-16}$
14	$-4.6157 \cdot 10^{-12}$	$-4.61(5) \cdot 10^{-12}$	$-4.49(1) \cdot 10^{-12}$
20	$-2.1085 \cdot 10^{-11}$	$-2.11(2) \cdot 10^{-11}$	$-1.99(1) \cdot 10^{-11}$
70	$-2.2051 \cdot 10^{-8}$	$-2.205(1) \cdot 10^{-8}$	$-8.86(1) \cdot 10^{-9}$
82	$-9.5886 \cdot 10^{-8}$	$-9.589(3) \cdot 10^{-8}$	$-2.51(1) \cdot 10^{-8}$

Table: g factor shifts due to hadronic VP[1].

- ALPHATRAP Accuracy $\sim 10^{-11} \longrightarrow$ observable effect

[1] E. Dizer, Bachelor Thesis, Heidelberg University (2020).

Hadronic g Factor Shift

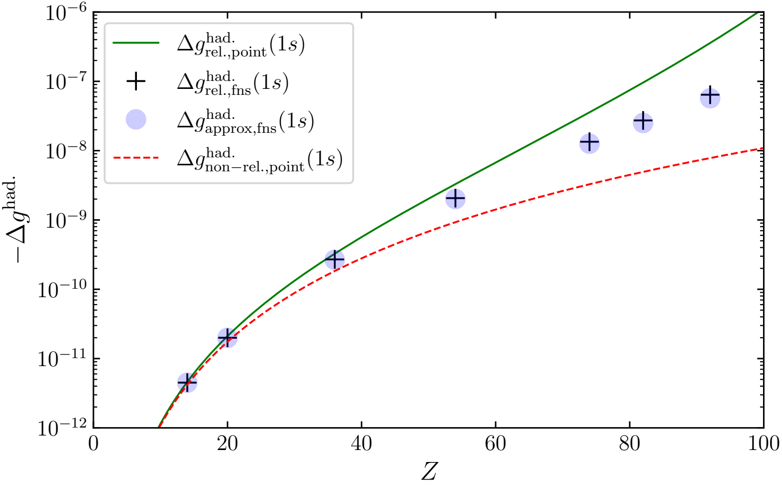

Figure: Comparison of numerical and analytical results.

Outline

1. One-Loop QED Corrections
2. Hadronic Vacuum Polarization
   - Hadronic Uehling Potential
   - Energy Level Correction
   - g Factor Correction
3. Two-Photon Excitations
   - Rabi Frequency
   - Cross Section
4. Outlook

Strong Laser Fields

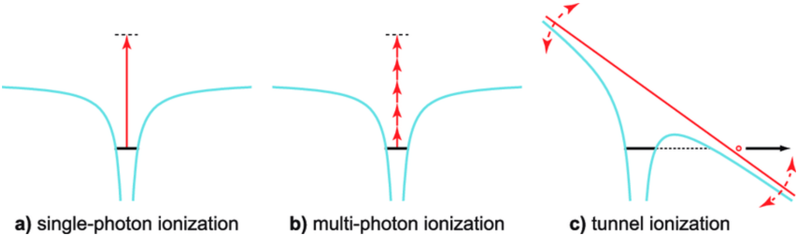

Figure: Ionization processes of atoms in strong laser fields.[1]

- Atoms get ionized in strong laser fields
- HCIs can be stable in stronger laser fields

[1] https://www.researchgate.net/figure/Basic-ionization-processes-in-atoms-a-\ In-single-photon-ionization-the-atom-is-ionized_fig7_321838945

Highly-Charged Ions

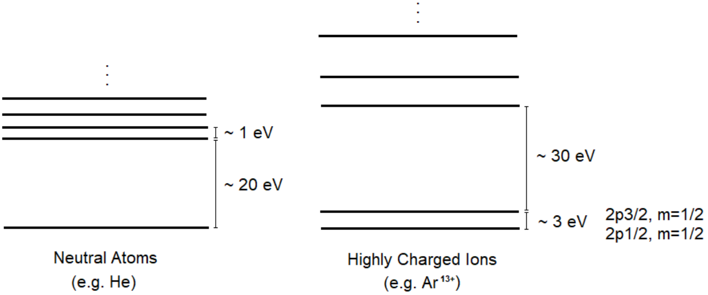

Figure: Level structure of neutral atoms compared to HCI.

- Energy levels of neutral atoms are very close to each other
- HCIs are better as approximate 2-level systems

Two-Photon Excitations

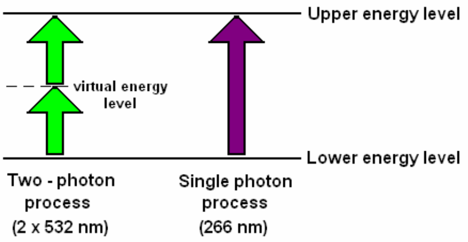

Figure: Schematic diagram of the two-photon absorption process.[1]

- Study Optical Response of effective Two-Level Systems
- Highly Charged Ions, Semiconductors, ...
- Deep Tissue Microscopy
- Second harmonic generation, parametric down conversion

[1] https://www.researchgate.net/figure/Schematic-diagram-of-the-two-photon-absorption-process-\exemplified-for-green-532-nm_fig1_228880601

Two-Photon Fluorescence

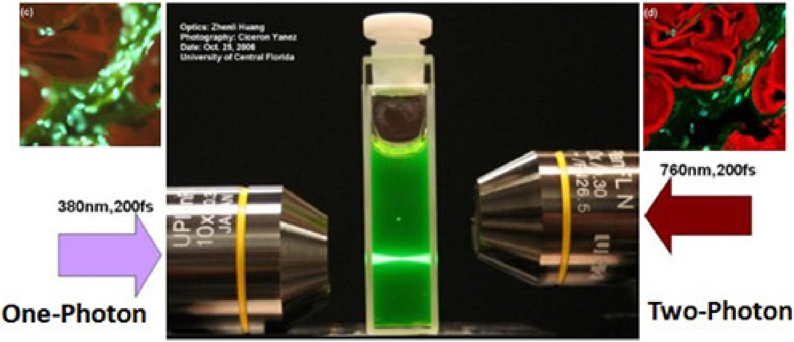

Figure: Comparison of one-photon and two-photon fluorescence.[1]

[1] https://manu56.magtech.com.cn/progchem/EN/abstract/abstract11942.shtml

Time-dependent Perturbation Theory

Time-dependent perturbation

$$i\hbar \frac{\partial}{\partial t}\psi(t, \boldsymbol{r}) = (H_0 + V(t))\psi(t, \boldsymbol{r}). \tag{13}$$

Time-depentent coefficients $\psi(t, \boldsymbol{r}) = \sum_n a_n(t)\phi_n$

$$i\hbar \dot{a}_m(t) = \varepsilon_m a_m(t) + \sum_n \langle m|V|n\rangle \, a_n(t). \tag{14}$$

Introduce $a_m(t) = c_m(t)e^{-i\varepsilon_m t/\hbar}$, $E_{nm} = \varepsilon_n - \varepsilon_m = \hbar\omega_{mn}$

$$i\hbar \begin{pmatrix} \dot{c}_1 \\ \dot{c}_2 \\ \vdots \\ \dot{c}_n \end{pmatrix} = \begin{pmatrix} V_{11} & V_{12}e^{iE_{12}t/\hbar} & \cdots & V_{1n}e^{iE_{1n}t/\hbar} \\ V_{21}e^{iE_{21}t/\hbar} & V_{22} & \cdots & V_{2n}e^{iE_{2n}t/\hbar} \\ \vdots & \vdots & \ddots & \vdots \\ V_{n1}e^{iE_{n1}t/\hbar} & V_{n2}e^{iE_{n2}t/\hbar} & \cdots & V_{nn} \end{pmatrix} \begin{pmatrix} c_1 \\ c_2 \\ \vdots \\ c_n \end{pmatrix} \tag{15}$$

Time-dependent Perturbation Theory

Light-atom interaction

$$V'_{nm} = V^{(-)}_{nm} e^{-i(\omega-\omega_{nm})t} + V^{(+)}_{nm} e^{i(\omega+\omega_{nm})t}. \tag{16}$$

Equations of motion for $c_1(t)$ and $c_2(t)$

$$i\hbar\dot{c}_1(t) = V'_{11}c_1(t) + V'_{12}c_2(t) + \sum_{j\geq 3} V'_{1j}c_j(t), \tag{17}$$

$$i\hbar\dot{c}_2(t) = V'_{21}c_1(t) + V'_{22}c_2(t) + \sum_{j\geq 3} V'_{2j}c_j(t). \tag{18}$$

Under perturbation, for $j \geq 3$

$$i\hbar c_j(t) = c_1(t)\int_0^t V'_{j1}dt' + c_2(t)\int_0^t V'_{j2}dt' + \dots . \tag{19}$$

Rabi Frequency

Effective Schrödinger equation for 2-photon transition ($\delta = 2\omega - \omega_{21}$)

$$i\hbar \begin{pmatrix} \dot{c}_1 \\ \dot{c}_2 \end{pmatrix} = \begin{pmatrix} \tilde{V}_{11} & \Omega e^{i\delta t} \\ \Omega^* e^{-i\delta t} & \tilde{V}_{22} \end{pmatrix} \begin{pmatrix} c_1 \\ c_2 \end{pmatrix}. \tag{20}$$

2-photon Rabi frequency

$$\Omega = \sum_{j\geq 3} \frac{V_{1j}^{(+)} V_{j2}^{(+)}}{-\hbar^2(\omega + \omega_{j2})} = \sum_{j\geq 3} \frac{\left\langle 1 \middle| \boldsymbol{\alpha} \cdot \hat{\epsilon}^* e^{-i\boldsymbol{k}\cdot\boldsymbol{r}} \middle| j \right\rangle \left\langle j \middle| \boldsymbol{\alpha} \cdot \hat{\epsilon}^* e^{-i\boldsymbol{k}\cdot\boldsymbol{r}} \middle| 2 \right\rangle}{-2\hbar^2(\omega + \omega_{j2})} \frac{Ie^2 c}{\varepsilon_0 \omega^2}. \tag{21}$$

- Physical constants $\varepsilon_0, e, c, \ldots$
- Laser intensity I and frequency $\omega = \omega_{21}/2$
- Level difference $\omega_{ij} = \omega_i - \omega_j$

Rabi Oscillations

$^{40}\mathrm{Ar}^{13+}$: $I = 5 \times 10^4$ W/cm^2 and $\hbar\omega = 1.4$ eV.
Lifetime of the excited state: $\tau = 9.6$ ms.

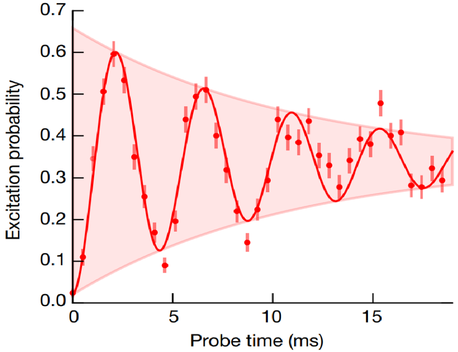

Figure: Rabi oscillations under 1-photon excitations in $^{40}\mathrm{Ar}^{13+}$.[1]

[1] P. Micke et al., Nature 578, 60–65 (2020).

Resonance Cross Section

2-photon excitation (TPE) cross section

$$\sigma = \left(\sum_{j \geq 3} \frac{\left\langle 1 \middle| \boldsymbol{\alpha} \cdot \hat{\epsilon}^* e^{-i\boldsymbol{k}\cdot\boldsymbol{r}} \middle| j \right\rangle \left\langle j \middle| \boldsymbol{\alpha} \cdot \hat{\epsilon}^* e^{-i\boldsymbol{k}\cdot\boldsymbol{r}} \middle| 2 \right\rangle}{(\omega + \omega_{j2})} \right)^2 \frac{e^4 c^2}{4\varepsilon_0^2 \Gamma}. \tag{22}$$

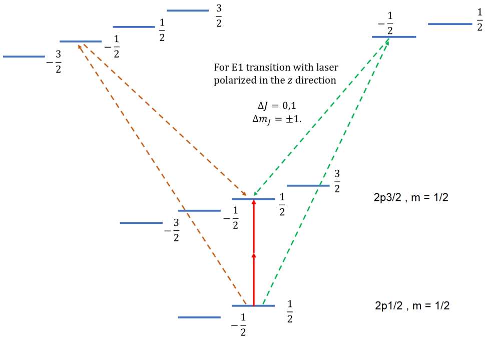

Resonance Cross Section

For comparison: Cross sections for two-photon microscopy:

$$\sigma = 1 \sim 300 \times 10^{-50}\ \text{cm}^4\text{s}.$$

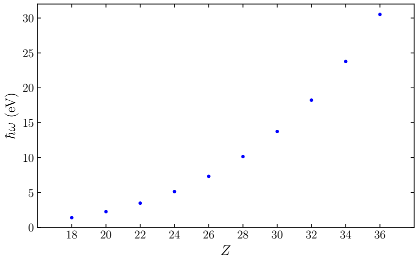

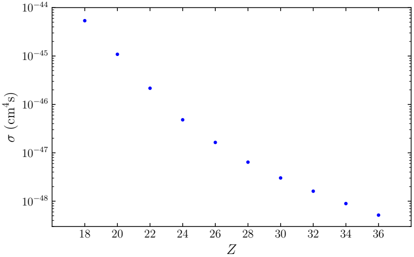

Figure: Laser frequency and TPE resonance cross section for different ions.

- Laser frequencies are in the optical to X-ray region
- XFEL photon flux $> 10^{24}$ ph/cm^2/s $\longrightarrow$ observable effect in HCIs

Outline

1. One-Loop QED Corrections
2. Hadronic Vacuum Polarization
   - Hadronic Uehling Potential
   - Energy Level Correction
   - g Factor Correction
3. Two-Photon Excitations
   - Rabi Frequency
   - Cross Section
4. Outlook

Outlook

Hadronic Vacuum Polarization:

- Hadronic Uehling potential can be applied to other systems
- Hadronic effects will be observable in future experiments

Two-Photon Excitations:

- Generalize to many-photon excitations
- Treatment beyond perturbation theory
- Calculate two-photon decay rate
- Experimental realization

Publications

Published:

- Hadronic Energy Shift (with S. Breidenbach et al.)[1]

In progress:

- Hadronic g Factor Shift (with Z. Harman)
- Two-Photon Excitations (with C. Lyu)

[1] S. Breidenbach et al., Physical Review A 106, 042805 (2022).

Thank you and stay healthy!